DOI: 10.1002/zaac.200800340

Tetramethoxy-λ^4-tellane and Tetrakis(2,2,2-trifluoroethoxy)-λ^4-tellane

Richard Betz, Martin Stapel, Maximilian Pfister, Felix W. Roeßner, Moritz M. Reichvilser, and Peter Klüfers*

München, Ludwig-Maximilians-Universität, Department Chemie und Biochemie

Received July 29th, 2008.

Dedicated to Professor Bernt Krebs on the Occasion of his 70th Birthday

Abstract. Two tetraalkoxy-λ^4-telluranes were prepared from tellurium tetrachloride and the sodium salts of methanol and 2,2,2-trifluoroethanol, respectively. Their molecular structures which were determined by single-crystal X-ray diffraction show dipolar intermolecular contacts. NBO analyses for the title compounds were conducted to assess the role of the stereochemically active lone pair on the tellurium atoms.

Keywords: Tellurium; Structure elucidation; Density functional calculations; NBO analysis; Bond theory

Introduction

Unlike its lower homologue selenium whose importance for the reproductive capability of many organisms has been established [1], tellurium has not been identified as an essential trace element. The metabolism of tellurium(IV) has not been demonstrated so far, yet it has been found that $Te(SR)_4$ compounds – that may form *in vivo* – easily undergo transformation to lower-oxidation-state tellurium compounds. In 1998, several tellurium(IV) compounds were found to show immunomodulating activity by interaction with cysteine protease [2]. As of today, polyols and carbohydrates which offer various bonding sites with their oxygen donor functions have not been tested as reasonable bonding partners for tellurium in living organisms and require a clarification of the fundamentals of this part of tellurium chemistry.

The synthesis of diol-derived *spiro*-λ^4/λ^6-tellanes may be conducted by exchange reactions with halogenides of tellurium in oxidation states +IV and +VI and diols in aprotic media [3, 4]. When considering carbohydrates as possible ligands for tellurium(IV), less reactive tetraalkoxytelluranes seem feasible as starting materials.

The first tetraalkoxy-λ^4-telluranes, $Te(OMe)_4$ and $Te(OEt)_4$, were prepared by *Meerwein* and *Bersin* from tellurium tetrachloride and their respective sodium alkoxides [5]. Some additional $Te(OR)_4$ compounds derived from sterically more demanding alcohols were prepared by *Denney* et al. following the same synthetic protocol [6]. Although the crystal structure of a mixed binuclear tellurium(IV) alkoxide compound, $Te(OMe)_4 \cdot ClTe(OMe)_3$, was determined by means of diffraction experiments on a single crystal [7], no molecular structure of a mononuclear tetraalkoxy-λ^4-tellurane is apparent in the literature. To rectify this lack of knowledge we herein report the molecular parameters of two mononuclear tetraalkoxytelluranes and interpret their structures in light of a computer-chemical analysis using the natural-bond orbital (NBO) approach. The compounds are also characterized by means of melting-point measurement, NMR, IR, Raman, UV/Vis, and mass spectrometry as well as elemental analyses.

Experimental Section

General Aspects

Tellurium tetrachloride was obtained from Aldrich (reagent grade) and used without further purification. Methanol (reagent grade) was supplied by Fluka and dried over molecular sieves (3 Å) prior to use. 2,2,2-Trifluoroethanol (reagent grade) was provided by ACROS and used as received. Sodium (reagent grade) was supplied by Fluka and used as received. Tetrahydrofuran (reagent grade) was obtained from Fluka and dried over molecular sieves (4 Å). Triethylamine (reagent grade) was obtained from Riedel-de-Haën and stored over potassium hydroxide pellets prior to use. A detailed description of the experimental procedure is given due to the partial scarce descriptions in the literature.

Physical measurements

NMR spectra were recorded in $CDCl_3$ at 25 °C (^1H, 400.2 MHz, TMS; ^{13}C, 100.6 MHz, TMS; ^{19}F, 376.5 MHz, $CFCl_3$; ^{125}Te, 126.3 MHz, Me_2Te) on a Jeol Eclipse 400 spectrometer. Mass spectra were recorded with a JEOL JMS-700 spectrometer. IR spectra were recorded with a Jasco FT-IR-460 Plus spectrometer with a Jasco Pike Miracle ATR unit. Raman spectra were measured with a Perkin Elmer 2000 NIR-FT spectrometer. UV/VIS spectra were measured with a CARY 50 Bio UV-Visible spectrometer in quartz glass cuvettes. Elemental analyses were done on a Vario Elementar

* Prof. Dr. Peter Klüfers
Department Chemie und Biochemie der Ludwig-Maximilians-Universität München
Butenandtstr. 5–13
D-81377 München, Germany
E-mail: kluef@cup.uni-muenchen.de

EL apparatus. The content of tellurium was determined by ICP-AES on a Varian-VISTA Simultan spectrometer. The melting points were obtained on a Büchi-540 apparatus and are uncorrected.

DFT calculations and NBO analyses

Geometry optimisation was performed with Gaussian03 [8] at the B3LYP/aug-cc-pVDZ-PP level of theory with very tight convergence criteria and an ultrafine integration grid. Twenty eight core electrons of tellurium have been replaced by a relativistic effective potential [9]. Frequency analyses were performed to ensure that the obtained structures represent minima on the potential energy hypersurface. Bonding was investigated by means of natural bond orbital analysis [10].

Crystallography

Intensity data for **1** and **2** were collected on an Oxford XCalibur 3 diffractometer (Mo-Kα radiation, λ = 0.71073 Å) at 200 K. The structure of **1** was solved using the program SIR-97 [11] and refined with SHELXL-97 [12]. The structure of **2** was solved using the program SHELXS-97 [12] and refined with SHELXL-97 [12]. The molecular diagrams were prepared with ORTEP III [13]. Intermolecular contacts were analyzed with Platon [14] and Mercury [15].

Preparation of tetramethoxy-λ^4-tellurane, $Te(OCH_3)_4$ **(1)**

Method A [6]: A three-necked flask (500 mL) equipped with two dropping funnels and a pressure equalising valve was charged under nitrogen with tellurium tetrachloride (6.44 g, 23.9 mmol) and tetrahydrofuran (51 mL) and cooled to −40 °C. After complete dissolution of the tellurium tetrachloride, methanol (3.93 mL, 3.11 g, 97.0 mmol) was added dropwise over 30 minutes. After the addition was completed a solution of triethylamine (13.52 mL, 9.82 g, 97.0 mmol) in tetrahydrofuran (39 mL) was added dropwise over the course of 30 minutes. A heavy, colourless solid separated from the reaction mixture immediately. The colourless suspension was then stirred for another 30 minutes with persistent cooling and separated from the solid by filtration under nitrogen. The solid was washed with tetrahydrofuran (15 mL) and the combined organic phases were concentrated under reduced pressure until a slight amount of solid started to separate from the reaction batch. Upon storage at −60 °C overnight, colour- and odourless needles were obtained, that were isolated by decantation and dried in a high vacuum, yield 3.48 g, 13.8 mmol, 58 %.

Method B [5]: In a three-necked flask (250 mL) equipped with a dropping funnel and a reflux-condenser with a pressure equalizing valve, sodium (4.50 g, 196 mmol) was dissolved under nitrogen in methanol (50 mL). After complete dissolution of the sodium, a solution of tellurium tetrachloride (12.75 g, 47.3 mmol) in methanol (15 mL) was added dropwise under cooling with a cold-water bath over the course of 20 minutes. A colourless-to-slightly-greyish solid separated from the reaction mixture. After the addition was completed the contents of the flask were heated under reflux for 60 minutes and separated from the solid by filtration under nitrogen. The solid was washed with methanol (10 mL) and the combined organic phases were evaporated to dryness under reduced pressure. A colour- and odourless powder was obtained, yield 7.85 g, 31.2 mmol, 65.9 %. **Melting point**: 67−70 °C. **Elemental analysis** found (calculated for $C_4H_{12}O_4Te$): C 15.09 % (19.08 %), H 3.68 % (4.80 %); problematic burning properties precluded correct results. **ICP-AES**, found (calculated for $C_4H_{12}O_4Te$): Te 50.48 % (50.69) %.

^{1}H NMR: δ = 3.79 (s). **^{13}C NMR:** δ = 51.8. **^{125}Te NMR:** δ = 1517. **MS** (CI^+, isobutane): 253 ($[M+H]^+$). **IR** (neat): ν = 2928 (w, CH_3), 2828 (w, CH_3), 2809 (w, CH_3), 1456 (w), 1437 (w), 997 (s), 683 (m) cm^{-1}. **Raman** (neat): ν = 2935 (29, CH_3), 2828 (16, CH_3), 2812 (25, CH_3), 1457 (8), 1439 (13), 1166 (2), 1051 (2), 1020 (3), 677 (5), 573 (100), 554 (47), 471 (8), 413 (38), 348 (13), 325 (10), 275 (8), 180 (9) cm^{-1}. **UV/Vis** (acetonitrile): no distinct absorption maxima in the range between 195.0 nm and 1100.0 nm; **UV/Vis** (cyclohexane): no distinct absorption maxima in the range between 195.0 nm and 1100.0 nm.

Preparation of tetrakis(2,2,2-trifluoroethoxy)-λ^4-tellurane, $Te(OCH_2CF_3)_4$ **(2)** [6]

In a three-necked flask (250 mL) equipped with a dropping funnel and a pressure equalizing valve sodium (2.89 g, 100 mmol) was suspended in tetrahydrofuran (50 mL) under nitrogen and 2,2,2-trifluoroethanol (7.19 mL, 10.00 g, 100 mmol) was added dropwise. After complete dissolution of the sodium the content of the flask was added dropwise with stirring to a pre-cooled solution (−40 °C) of tellurium tetrachloride (6.89 g, 24.0 mmol) in tetrahydrofuran (30 mL) over the course of 30 minutes upon which a heavy colourless solid separated from the reaction mixture. After the addition was completed the colourless suspension was stirred for another 30 minutes with persistent cooling and separated from the solid by filtration under nitrogen. The solid was washed with tetrahydrofuran (15 mL), the combined organic phases were concentrated under reduced pressure and the remainder was distilled under reduced pressure (p = 1.3 × 10^{-1} mbar, T = 64 °C at top of distillation head). A yellow liquid with a pungent garlic-like odour was obtained that solidifies upon storage at 4 °C, yield 8.00 g, 15.3 mmol, 64 %. **Melting point**: 30−31 °C. **Elemental analysis** found (calculated for $C_8H_8F_{12}O_4Te$): C 17.30 % (18.35 %), H 1.54 % (1.54 %); problematic burning properties precluded correct results. **ICP-AES**, found (calculated for $C_8H_8F_{12}O_4Te$): Te 25.11 % (24.36) %; the sensitivity of the compound to hydrolysis hampered the preparation of a sample.

^{1}H NMR: δ = 4.38 (q, J = 8.5 Hz). **^{13}C NMR:** δ = 124.1 (q, J = 279 Hz, CF_3), 62.1 (q, J = 35.6 Hz, CH_2). **^{19}F NMR:** δ = −76.0 (t, J = 8.5 Hz, CF_3). **^{125}Te NMR:** δ = 1460. **MS** (CI^+, isobutane): 525 ($[M+H]^+$). **IR** (neat): ν = 2971 (w, CH_2), 2946 (w, CH_2), 2882 (w, CH_2), 1736 (w), 1455 (w), 1406 (w), 1370 (w), 1270 (s), 1146 (s), 1050 (s), 951 (s), 835 (m), 710 (m), 676 (m), 629 (w), 616 (w), 602 (m) cm^{-1}. **Raman** (neat): ν = 2929 (40, CH_2), 1457 (56), 836 (100), 614 (72), 608 (92), 538 (84), 367 (64), 354 (76) cm^{-1}. **UV/Vis** (acetonitrile): 426.5, 452.6 nm; **UV/Vis** (cyclohexane): 450.0 nm.

Crystal structure determination

1: $C_4H_{12}O_4Te$, M_r = 251.74 g mol^{-1}, colourless platelet, 0.37 × 0.10 × 0.05 mm, triclinic, P −1, a = 7.1920(14), b = 8.2290(15), c = 8.3120(18) Å, α = 64.62(2), β = 70.141(19), γ = 71.365(17)°, V = 409.17(16) Å^3, Z = 2, ρ = 2.043 g cm^{-3}, T = 200(2) K, μ(MoK$_\alpha$) = 3.589 mm^{-1}, analytical absorption correction, Oxford Xcalibur 3, θ range = 4.57−24.03°, 1796 refls., 1290 independent and used in refinement, 1189 with $I \geq 2\sigma(I)$, R_{int} = 0.0663, mean $\sigma(I)/I$ = 0.0440, 87 parameters, $R(F_{obs})$ = 0.0382, $R_w(F^2)$ = 0.0996, S = 1.095, min. and max. residual electron density: −1.170/1.809 e Å^{-3}, max. shift/error = 0.001.

2: $C_8H_8F_{12}O_4Te$, M_r = 523.74 g mol^{-1}, yellow block, 0.35 × 0.29 × 0.21 mm, triclinic, P −1, a = 8.2905(17), b = 9.5403(13), c =

10.081(2) Å, α = 78.425(14), β = 81.671(17), γ = 85.173(14)°, V = 771.6(2) Å^3, Z = 2, ρ = 2.254 g cm^{-3}, T = 200(2) K, μ(MoK$_\alpha$) = 2.075 mm^{-1}, analytical absorption correction, Oxford XCalibur 3, θ range = 3.94−27.56°, 9888 refls., 3413 independent and used in refinement, 2879 with $I \geq 2\sigma(I)$, R_{int} = 0.0591, mean $\sigma(I)/I$ = 0.0505, 227 parameters, $R(F_{obs})$ = 0.0242, $R_w(F^2)$ = 0.0557, S = 1.016, min. and max. residual electron density: −0.793/1.243 e Å^{-3}, max. shift/error = 0.001.

Crystallographic data have been deposited with the Cambridge Crystallographic Data Centre: **1**: 673447, **2**: 673448. Copies of the data can be obtained free of charge on application to the Director, CCDC, 12 Union Road, Cambridge CB2 1EZ, UK (Fax: int.code +(1223)336-033; e-mail for inquiry: **file-server@ccdc.cam.ac.uk**).

Results and Discussion

Crystal structure analysis

Tetramethoxy-λ⁴-tellurane (**1**) was prepared by two different synthetic protocols found in the literature, in one-step procedures from tellurium tetrachloride and methanol in the presence of triethylamine [6], or from tellurium tetrachloride and sodium methoxide [5].

The results of a single-crystal X-ray study show four methoxy groups attached to the tellurium atom (Figure 1). The seesaw-shaped molecules show longer Te-O distances along the molecular axis and shorter ones in the equatiorial plane (for selected average bond lengths and angles see Table 1).

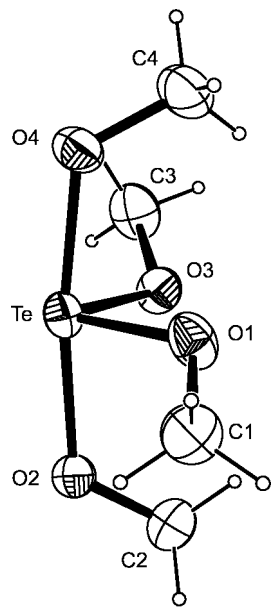

Figure 1 Structure of Te(OMe)$_4$ (**1**) (50 % probability ellipsoids). For selected average bond lengths and angles *cf.* Table 1. Selected individual bond lengths and angles: Te-O1 1.928(5), Te-O2 2.052(5), Te-O3 1.920(4), Te-O4 2.028(5) Å, O4-Te-O2 171.42(18), O3-Te-O1 90.0(2)°.

The values for Te-O distances in **1** are similar to those observed for a pinacol-derived *spiro*-tellurane Te(C$_6$H$_{12}$O$_2$)$_2$, yet the axial bonds are found to be slightly longer and the equatorial bonds to be slightly shorter in **1** [16]. Bigger differences are observed for the O$_{ax}$-Te-O$_{ax}$ angle and for the O$_{eq}$-Te-O$_{eq}$ angle − the first one being much closer to linearity than in the spiro compound, the latter one being more compressed to nearly 90°.

Table 1 Comparison of selected averaged experimental bond lengths and angles (XRD) for Te(OCH$_3$)$_4$ (**1**) and Te(OCH$_2$CF$_3$)$_4$ (**2**) with the corresponding parameters calculated at the B3LYP/aug-cc-pVDZ-PP level of theory (DFT).

	1		**2**	
	XRD	DFT	XRD	DFT
d(Te-O$_{ax}$)/Å	2.04	2.04	2.03	2.05
d(Te-O$_{eq}$)/Å	1.92	1.99	1.91	1.98
<(O$_{ax}$-Te-O$_{ax}$)/°	171.4	173.4	163.6	168.7
<(O$_{ax}$-Te-O$_{eq}$)/°	87.0	87.9	84.9	86.3
<(O$_{eq}$-Te-O$_{eq}$)/°	90.0	102.1	95.5	98.5

Tetrakis(2,2,2-trifluoroethoxy)-λ⁴-tellurane (**2**) was prepared according to a published procedure upon the reaction of tellurium tetrachloride and the sodium salt of 2,2,2-trifluoroethanol [6]. An X-ray analysis of **2** yielded a similar picture for the tellurium atom's coordination environment (Figure 2). Te-O bonds in **2** are shorter than in **1**. The only exception is observed for one of the axial bonds which is elongated possibly due to intermolecular Te-O contacts (see below). The angle between the axial positions shows a larger deviation from a linear arrangement of atoms than in **1**, the O$_{eq}$-Te-O$_{eq}$ angle is found slightly enlarged (for selected average bond lengths and angles, see Table 1).

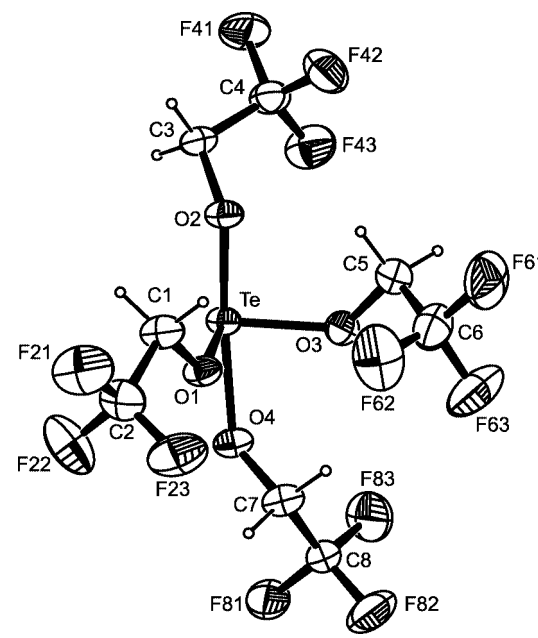

Figure 2 Structure of Te(OCH$_2$CF$_3$)$_4$ (**2**) (50 % probability ellipsoids). For selected average bond lengths and angles *cf.* Table 1. Selected individual bond lengths and angles: Te-O1 1.9004(18), Te-O2 2.0118(15), Te-O3 1.9168(18), Te-O4 2.0391(16) Å, O4-Te-O2 163.56(7), O3-Te-O1 95.51(8)°.

An analysis of the crystal structures of **1** and **2** shows intermolecular contacts as a prominent feature. As was observed for the pinacol-derived *spiro*-λ^4-tellurane [16] and a pyrocatechol-derived *spiro*-λ^4-tellurane [17], Te-O contacts whose ranges fall up to 0.7 Å below the sum of the vander-Waals radii of the corresponding atoms (3.60 Å for Te-O [18]) are present. In **1**, a pair of longer and shorter Te-O contacts connects the molecules to infinite chains along [100]. Only oxygen atoms in axial positions participate in the formation of these contacts. The coordination polyhedron around the tellurium atom in **1** is extended to a heavily distorted octahedron (Figure 3). A different picture is observed for **2**: possibly due to the steric demand of the 2,2,2-trifluoroethoxy groups, the formation of centrosymmetric dimers is observed (Figure 4). The coordination polyhedron around the Te atoms resembles that of a distorted trigonal bipyramid. The exclusive dimeric motif has not been observed so far, comparable Te(IV)-oxygen compounds furnish the formation of Te-O chains with one [17] or two [16] dipolar contacts between adjacent molecules. The coordination sphere around the tellurium atom either is extended to a distorted trigonal bipyramid [17] or to an octahedron [16, 19], the latter case including disordered solvent molecules apparent in the crystal structure.

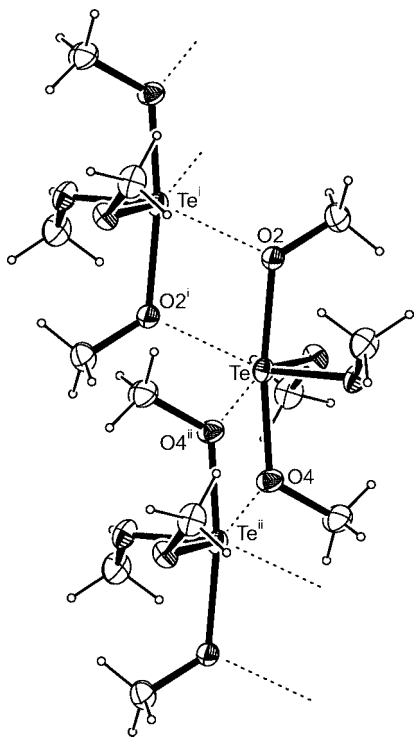

Figure 3 Intermolecular contacts in the crystal strcuture of $Te(OCH_3)_4$ (**1**) (viewed along [010]). Selected distances and angles: Te-O2^{i} 2.815(5), Te-O4^{i} 2.880(6) Å, O2^{i}-Te-O4^{ii} 112.2(2)°. Symmetry operators: ^{i} $-x$, $-y + 2$, $-z$; ^{ii} $-x + 1$, $-y + 2$, $-z$.

NMR properties and hydrolytic stability

^{13}C NMR spectra of crystals of **1** dissolved in $CDCl_3$ show only one resonance. A comparison with the chemical shift of neat methanol in the same solvent shows that upon bonding to tellurium the carbon resonance is shifted about 1.7 ppm downfield. Proton spectra of the same sample showed a single resonance. The downfield shift for the protons in comparison to neat methanol is about 0.37 ppm.

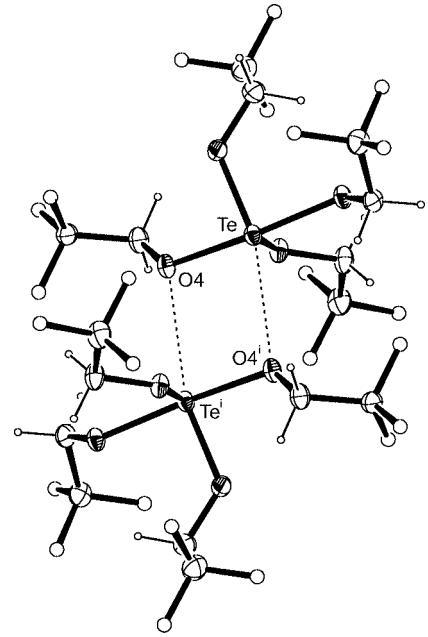

Figure 4 Intermolecular contacts in the crystal strcuture of $Te(OCH_2CF_3)_4$ (**2**) (viewed along [100]). Selected distances and angles: Te-O4^{i} 2.804(2) Å, O4-Te-O4^{i} 78.41(6), Te-O4-Te^{i} 101.59(6)°. Symmetry operator: ^{i} $-x + 1$, $-y$, $-z + 1$.

When crystalline **2** is dissolved in $CDCl_3$ two quartets are observed in ^{13}C NMR spectra. A comparison of the chemical shifts with the corresponding ones in pure 2,2,2-trifluoroethanol shows a downfield shift of the oxygen-bonded carbon atoms of 0.9 ppm and 0.3 ppm for the trifluoromethyl group. C-F coupling constants remain essentially unaffected by the bonding to tellurium. ^{1}H NMR spectra of the same sample show a downfield shift of up to 0.42 ppm. ^{19}F NMR spectra show a slight upfield shift of around 2 ppm. The number of signals is in agreement with rapid ligand reorganisation. Temperature-dependent NMR spectroscopy had already been performed earlier and showed no signs of halting this process [6].

The ^{125}Te NMR spectra of **1** as well as of **2** recorded in $CDCl_3$ show one resonance each whose chemical shift is in accordance with the values reported in the literature for these particular and comparable $Te(OR)_4$ compounds [6].

1 and **2** are unstable against hydrolysis: upon addition of several drops of water to an NMR sample a flocculent colourless precipitate immeditaley separated from the solution clogging the entire NMR tube.

DFT results and NBO analyses

Results of the geometry optimisation procedure are compiled in Table 1. A particularly large difference between the

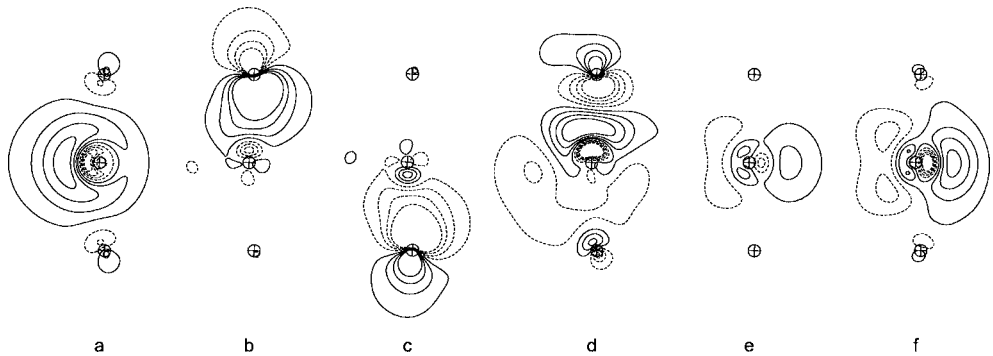

Figure 5 Isocontour plots of selected natural bond orbitals in **1**. Isolines are drawn at 0.03, 0.08, 0.13 and 0.18. The drawing plane contains both axial oxygen atoms and the central selenium atom (crossed circles). (a) lone pair on Te, (b, c) Te-O_{ax} bonding s orbitals, (d) Te-O_{ax} antibondingσ^* orbital, (e) Te-O_{eq} bonding s orbitals, (f) Te-O_{eq} antibonding σ^* orbitals.

calculated data and the X-ray result is found for the O_{eq}-Te-O_{eq} angle in **1**. In the solid state, this angle is markedly compressed with respect to the DFT result which may be caused by the two intermolecular Te-O contacts that are not considered in the calculation.

In a molecular-orbital approach, axially oriented p orbitals of Te and O contribute to several canonical MOs in the sense of a 4e-3c bond. The molecular orbital associated with the Te lone pair is characterised by a dominant contribution of the Te 5s atomic orbital.

Similar results were obtained by using a localised-orbital approach. In the framework of natural bond orbital (NBO) analysis, the Te-O bonds are markedly heteropolar, the relatively small contribution of the tellurium orbitals being dominated by 5p AOs. Thus the equatorial bonds (18.5 % Te character) resemble an $s^{0.07}p^{0.83}d^{0.09}$ hybridisation, whereas an $s^{0.11}p^{0.67}d^{0.22}$ hybridisation is assigned to the even more polar axial bonds (11.9 % Te character). In agreement with the MO approach, the lone pair on tellurium is found to show an $s^{0.82}p^{0.18}$ hybridisation. The d-AO contribution to the hybrid orbitals stems exclusively from low-populated Rydberg orbitals which, in conjunction with the highly ionic character of the Te-O bonds, leads to no actual valence-shell d-orbital occupation. Accordingly, a natural population analysis (NPA) reveals an overall Te-AO contribution where the d participation does not exceed a value that might be expected if diffuse functions are provided ($s^{1.76}p^{1.94}d^{0.03}$).

Figure 5 shows isocontour plots of selected natural orbitals of tetramethoxy-λ⁴-tellurane (**1**). A second-order perturbation-theory analysis reveals that there are energetically favourable $\sigma-\sigma^*$ interactions (negative hyperconjugation) between occupied Te-O bonding orbitals and the adjacent antibonding Te-O orbitals. As expected, due to their approximated collinearity, the two possible interactions between an axial bonding (b) and the opposed antibonding Te-O orbitals (d) give rise to the largest two-electron stabilization energies, which are 202 kJ mol^{-1}. The corresponding energy for each of the four possible interactions between equatorial Te-O bonds (e) and antibonding axial orbitals (d) is 148 kJ mol^{-1}. The third possible type of interaction, which gives rise to two electron stabilisation energies of 104 kJ mol^{-1}, is a delocalisation from axial bonding Te-O orbitals (b,c) to equatorial antibonding orbitals (f).

As a result, the bonding situation on **1** and **2** might be described by assuming a nearly non-hybridised Te atom forming two 2e-2c Te-O bonds to the O atoms in the equatorial plane and a 4e-3c Te-O bond along the linear O-Te-O fragment. The lone pair is located mainly in the Te 5s orbital but is decentered by a considerable 5p contribution. Accordingly, the O_{ax} atoms are bent away from the thus weakly stereochemically active Te lone pair.

Conclusions

The X-ray analysis of tetramethoxy-λ⁴-tellurane and tetrakis(2,2,2-trifluoroethoxy)-λ⁴-tellurane provides information about the coordination environment and the bonding of the tellurium atom. An NBO treatment shows the highly heteropolar character of the Te-O bonds and the dominant s character of the tellurium lone pair. With this structural knowledge at hand, the optimum O-atom pattern that has to be provided by a chelating carbohydrate ligand is obvious.

References

[1] D. Behne, H. Weiler, A. Kyriakopoulos, *J. Reprod. Fertil.* **1996**, *106*, 291−297.
[2] A. Albeck, H. Weitman, B. Sredni, M. Albeck, *Inorg. Chem.* **1998**, *37*, 1704−1712, and cited literature.
[3] M. Allan, A. F. Janzen, C. J. Willis, *Can. J. Chem.* **1968**, *46*, 3671−3677.
[4] G. W. Fraser, G. D. Meikle, *J. Chem. Soc. Dalton Trans.* **1975**, 1033−1036.
[5] H. Meerwein, T. Bersin, *Liebigs Ann. Chem.* **1929**, *476*, 113−150.
[6] D. B. Denney, D. Z. Denney, P. J. Hammond, Y. F. Hsu, *J. Am. Chem. Soc.* **1981**, *103*, 2340−2347.
[7] H. Fleischer, D. Schollmeyer, *Inorg. Chem.* **2001**, *40*, 324−328.
[8] M. J. Frisch, G. W. Trucks, H. B. Schlegel, G. E. Scuseria, M. A. Robb, J. R. Cheeseman, J. A. Montgomery, Jr., T. Vreven,

K. N. Kudin, J. C. Burant, J. M. Millam, S. S. Iyengar, J. Tomasi, V. Barone, B. Mennucci, M. Cossi, G. Scalmani, N. Rega, G. A. Petersson, H. Nakatsuji, M. Hada, M. Ehara, K. Toyota, R. Fukuda, J. Hasegawa, M. Ishida, T. Nakajima, Y. Honda, O. Kitao, H. Nakai, M. Klene, X. Li, J. E. Knox, H. P. Hratchian, J. B. Cross, V. Bakken, C. Adamo, J. Jaramillo, R. Gomperts, R. E. Stratmann, O. Yazyev, A. J. Austin, R. Cammi, C. Pomelli, J. W. Ochterski, P. Y. Ayala, K. Morokuma, G. A. Voth, P. Salvador, J. J. Dannenberg, V. G. Zakrzewski, S. Dapprich, A. D. Daniels, M. C. Strain, O. Farkas, D. K. Malick, A. D. Rabuck, K. Raghavachari, J. B. Foresman, J. V. Ortiz, Q. Cui, A. G. Baboul, S. Clifford, J. Cioslowski, B. B. Stefanov, G. Liu, A. Liashenko, P. Piskorz, I. Komaromi, R. L. Martin, D. J. Fox, T. Keith, M. A. Al-Laham, C. Y. Peng, A. Nanayakkara, M. Challacombe, P. M. W. Gill, B. Johnson, W. Chen, M. W. Wong, C. Gonzalez, J. A. Pople, *Gaussian 03, Revision B.03/D.01.*, Gaussian, Inc., Wallingford CT, **2004**.

[9] K. A. Peterson, D. Figgen, E. Goll, H. Stoll, M. Dolg, *J. Chem. Phys.* **2003**, *119*, 11113−11123.

[10] E. D. Glendening, J. K. Badenhoop, A. E. Reed, J. E. Carpenter, J. A. Bohmann, C. M. Morales, and F. Weinhold, *NBO 5.G*, Theoretical Chemistry Institute, University of Wisconsin, Madison, **2001**.

[11] A. Altomare, M. C. Burla, M. Cavalli, G. L. Giacovazzo, A. Gagliardi, A. G. G. Moliterni, G. Polidori, R. Spagna, *SIR97, A New Tool For Crystal Structure Determination and Refinement*, *J. Appl. Cryst.* **1999**, *32*, 115−119.

[12] G. M. Sheldrick, *Acta Crystallogr.* **2008**, *A64*, 112−122.

[13] M. N. Burnett, C. K. Johnson, *ORTEP III, Oak Ridge Thermal Ellipsoid Plot Program for Crystal Structure Illustrations*, Oak Ridge National Laboratory Report ORNL-6895, **1996**.

[14] A. L. Spek, *PLATON, A Multipurpose Crystallographic Tool*, Utrecht University, The Netherlands, **2007**.

[15] CCDC, *Mercury 1.4.2 (Build 2)*, CCDC **2001−2007**.

[16] R. O. Day, R. R. Holmes, *Inorg. Chem.* **1981**, *20*, 3071−3075.

[17] O. Lindqvist, *Acta Chem. Scand.* **1967**, *21*, 1473−1483.

[18] A. Bondi, *J. Phys. Chem.* **1964**, *68*, 441−451.

[19] S. Yosef, M. Brodsky, B. Sredni, A. Albeck, M. Albeck, *ChemMedChem* **2007**, *2*, 1601−1606.

